Frequency response analysis of soil-structure interaction for concrete gravity dams

A. De Falco[1], M. Mori*[1], G. Sevieri[2]
[1]Dept. of Energy, Systems, Territory and Construction Engineering, Pisa Univ. (Italy),
[2]Dept. of Civil and Environmental Engineering, Florence Univ. (Italy).
*Corresponding author: largo L. Lazzarino, 1 - 56126 Pisa, morimatteo123@gmail.com

Abstract: The seismic evaluation of existing dams is a major issue that was even more highlighted by the recent events in Italy. In this regard, researchers and engineers need a reliable and quick tool to assess the complex behaviour of the dam – reservoir – soil system.
COMSOL Multiphysics® [1] is able to effectively perform a coupled study in the frequency domain by using both Structural Mechanics and Acoustic modules and offers the possibility to simulate the unboundedness of the half space terrain and reservoir.
In this paper the soil-structure interaction for concrete gravity dams is considered, investigating its effect on the dynamic response of a 2D system under earthquake excitation. More specifically, the advantages of considering the semi unbounded domains will be shown. To this purpose the results in terms of structural response will be obtained under different boundary conditions and modelling approaches.

Keywords: *Perfectly Matched Layer, concrete gravity dams, radiation damping, soil-structure interaction.*

1. Introduction

During earthquake shaking the dam-reservoir-foundation system must be considered as a coupled system. The consequences rising from these interactions could result in relevant amplifications in terms of stresses within the dam body, in respect to the ones that are obtained from traditional simplified analyses. To date the models seldom take into account both effects, because of the lack of adequate numerical implementations or computational resources required by three dimensional detailed models.
In this paper the soil interaction effect is analyzed. It is described in the literature to have two main components: kinematic interaction and inertial interaction [2]. The former is governed by soil flexibility, which modifies the frequency response of the system, usually shifting it to lower frequencies. The latter is generated by the elastic waves that develop under dynamic loads, promoting the energy transport through the soil volume. Such a phenomenon, that carries energy away from the structure, is often referred as *"radiation damping"*.
In this work, the interaction has been investigated and the unboundedness of the half space domain has been analyzed in order to turn the radiation damping effect in term of equivalent material damping coefficient.

2. State of the art

In general, the soil effect on the seismic behavior of buildings is seldom explicitly taken into account in finite element models. More often, in order to overcome the difficulties involved in modeling soil-structure interaction, code-provided response spectra depending on suitable soil categories are used. The particular characteristics of the retaining structures do not allow using methods commonly applied to ordinary buildings, so dam earthquake safety assessment requires the direct modeling of soil structure interaction.
In the literature two contributions are relevant in approaching the problem of soil-structure interaction, those by Wilson [2] and Wolf [3], [4]. Wilson describes the *"massless foundation"* method, basing on the consideration that the recorded ground motions are acquired at the terrain surface where the response has already experienced the effects of the soil. Massless foundation model, proposed by Clough in 1980 [5], has been utilized extensively in seismic analysis of dam-foundation problems. The soil is therefore modelled only in terms of flexibility and by imposing the recorded displacement at the boundaries of the domain, disregarding the inertial interaction. In the massless model, the wave velocity in foundation becomes infinite, so the input motion reaches instantaneously the base of the dam and the structure takes all kinetic energy. These assumptions seem in general unrealistic [6].
The unboundedness of the terrain is first considered by Lamb [7] in its classical problem of a point load on a half space, for which he provides an analytical solution. Wolf [4], on the other hand, provides a

formulation for appropriate spring-dashpot coefficients and boundary conditions.
More recently, soil-structure interaction for concrete retaining structures is addressed by many authors searching for a reliable simulation of wave propagation in a semi-infinite medium, modelling the far field part of the foundation. Some methods worth noting are Lysmer boundary conditions [8], hyperelements [9], infinite elements [10], [11] rational boundary conditions [12], boundary element method [13], scaled boundary element method [14] and high order non-reflecting boundary conditions [15].
The Perfectly Matched Layer (PML) is a technique able to absorb incident waves under any angle and frequency, preventing them from returning back to the medium after incidence to the model boundaries. It was first introduced by Berenger in 1994 [16] and was successively applied to many different physical problems. It comes to a complex coordinate stretching of the domain that introduces a decay of the oscillation without any reflection in the source domain, simulating a perfectly absorbing material.
In this work, PML is used to simulate the unboundedness of both solid and fluid domains.

3. COMSOL Models

COMSOL offers the suitable tools to perform accurate fully coupled FSI analysis and to simulate infinite extension domains. The fluid subsystem is accurately simulated with the Helmoltz equation derived from the full Navier-Stokes equation in the hypothesis of small vibrations and neglecting viscosity; the dam and soil domains are modeled by applying the standard Solid Mechanics equations. In this work, the PML functionality implemented in COMSOL is used to simulate the unboundedness of the terrain half-space and the upstream reservoir.
The study of interaction phenomena is performed in the frequency domain on several plane strain models of an Italian concrete gravity dam 65 meters tall. In this context, the effect of considering the coupling and the unboundedness of the fluid and solid domains is evaluated. As shown in figures 1, 2 and 3, three models were set-up. A first reference model simulates the dam on rigid terrain, a second model includes the standard massless foundation in a bounded region and a third model accounts for massed foundation as an unbounded half-space. In this latter case, PMLs were applied at the bottom and on the sides. In all cases, the mesh is made up of default second-order serendipity elements whose number is 453 for model 1, 3146 for model 2 and 3692 for model 3. The three models share the same plane-strain settings and material settings, as reported in Table 1.

	Concrete	*Foundation rock*
Density **ρ** *(kg/m³)*	2450	2300
Young modulus **E** *(MPa)*	20500	22000
Poisson modulus **ν**	0.2	0.2
Damping coefficient **ξ**	0.05	0.05

Table 1. Material parameters.

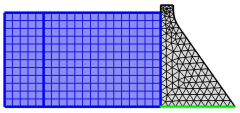

Figure 1. Model 1: Rigid soil.

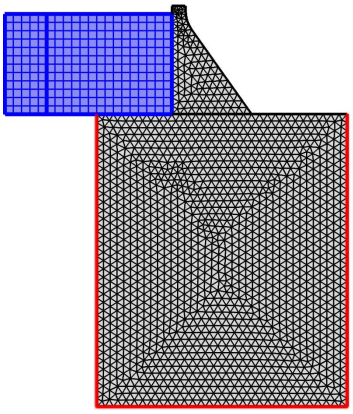

Figure 2. Model 2. Massless model.

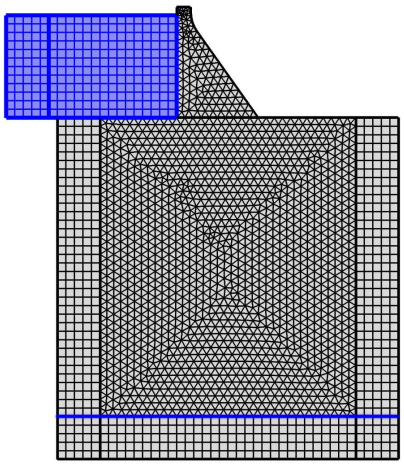

Figure 3. Model 3. Infinite terrain model.

The PML mesh has to be assigned so that the element sides are directed along the radiation. In addition, according to Kuhlemeyer and Lysmer [17], for accurate representation of wave transmission through the model, the spatial element size is selected to be smaller than approximately one-eighth of the wavelength associated with the highest frequency component of the input wave. In this case, the

frequency sweep ranges between 0 Hz and 25 Hz and the maximum mesh size is 5 m.
In order to make the three models comparable to each other, the same horizontal harmonic acceleration has to be provided at the base of the dam.
As for boundary conditions, in models 1 and 2, an horizontal acceleration with peak amplitude of 1m/s^2 is applied to the green and the red contours, respectively. Unfortunately, the application of PMLs on the exterior boundaries of the terrain model makes them no longer available for a displacement boundary condition. Similarly, by applying the cinematic condition to the interface between the dam and the soil, the outgoing waves are blocked since the field variable ***u*** is fixed. This problem is overcome by the *"global equation"* functionality implemented in COMSOL. In particular, leaving the displacement unconstrained, a distributed force load was applied at the PML interface and its value was "tuned", frequency by frequency, by a global equation, enforcing an average unit acceleration condition at the dam base. The peak value of the horizontal load must satisfy the following global equation

$$aveop1(solid.accX)-1=0 \qquad (1)$$

This setting makes the three models comparable.
The analysis was conducted with empty reservoir, and in the presence of water. The basin is simulated using both the simplified Westergaard [18] added mass model (Figure 4) and the full acoustic coupling. In this latter case, the acoustic water domain has the PML at the upstream side, the zero pressure boundary condition at the free surface and the rigid boundary condition at the bottom. Base shear and crest acceleration responses have been obtained for a total of nine cases, in order to detect the soil effect.

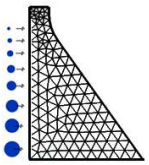

Figure 4. The added masses model to simulate the hydrodynamic effect of the basin.

It can be observed (figures 5 and 6) that the massless terrain model (red curves) compared with the rigid soil model (green curves), introduces a wide, spurious amplification, particularly in the range between 7 to 11 Hz, while lowering the peak frequencies and increasing their values. On the other hand, the infinite terrain model (blue curves), besides a downward frequency shift in respect to the rigid soil model (green curves), displays a noticeable reduction of the peak response, due to radiation damping.

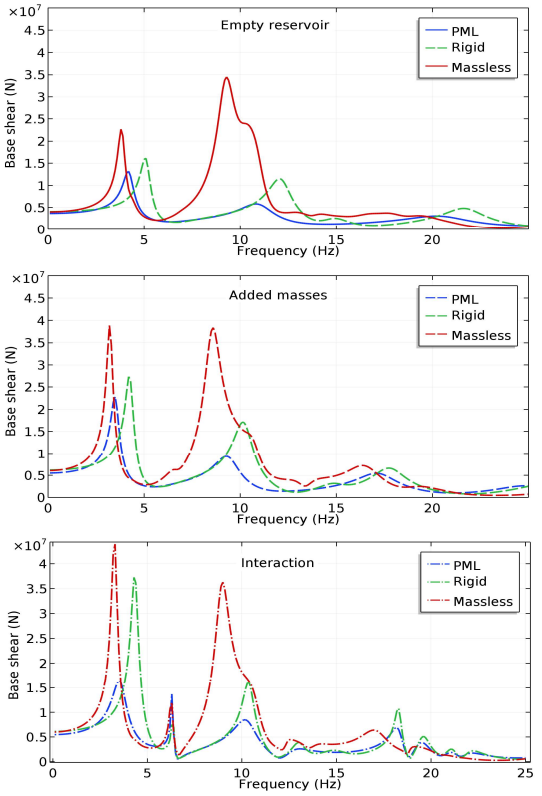

Figure 5. Response curves for the base shear.

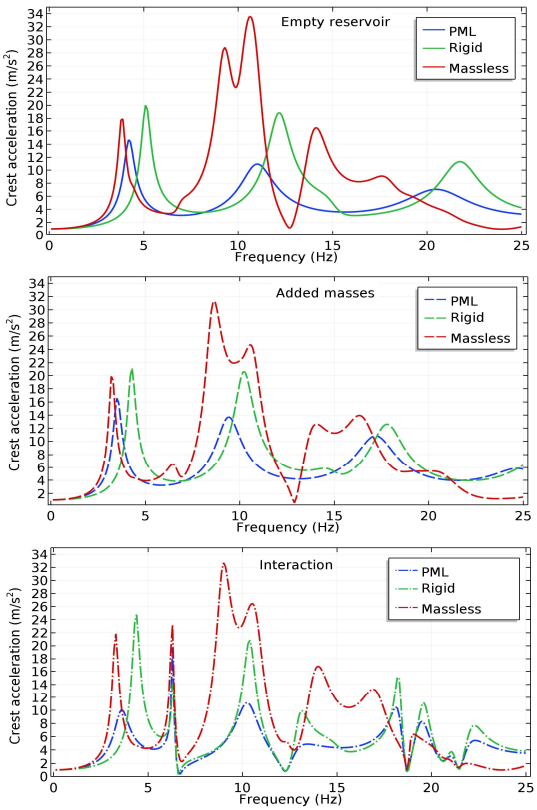

Figure 6. Response curves for the crest acceleration.

The infinite domain model does not introduce any spurious peaks. The observed behaviour is displayed in all three cases of empty reservoir, added masses and full interaction, for both base shear and crest displacement response. In the case of fluid- structure interaction, the first eigenmode of the reservoir remains well visible, at

$$f_r = \frac{c}{4h} = \frac{1483\ m/s}{4{\cdot}60\ m} = 6.17\ Hz, \qquad (2)$$

where c is the sound velocity in the water and h is the height of the basin. The amplitude of its peak is lower for the total base shear, than for the crest acceleration. As a side note, the reservoir driven resonances can be easily identified, due to their very narrow bandwidth and their frequency location.

In Figure 7 the fluid pressure and the solid displacement colour maps for the models 2 and 3 are reported under a 10Hz frequency excitation. The streamlines represent the acoustic energy flux within the fluid and the mechanical energy flux within the solid that originate from the bottom of the soil domain. The mechanical energy flux I is defined by

$$\mathrm{I} = \frac{1}{2}\mathrm{Re}\left(-\sigma_{ij} v_{ij}^{*}\right), \qquad (3)$$

where σ is the stress tensor and v the velocity vector. A remarkable difference between the two systems can be observed. The massless model displays a circulatory streamlines pattern, without a defined incoming wave front. In this case the streamlines become curly when frequency increases. The infinite massed terrain model, instead, displays a well-defined energy flux direction, as well as the lower amount of energy transmitted to the basin in respect to the former case.

4. Parametric analysis

In order to better understand the effect of the change in stiffness and density of soil and concrete, a parametric study is performed on a model with empty reservoir, that allows better isolating the terrain contribution.

In the figures 8 and 9 the response curves in term of base shear and crest displacement, varying the soil stiffness E_g and density ρ_g are shown. The corresponding parameters of concrete are kept unchanged (Table 1). The graphs are expressed in function of the logarithm of the ratio between the variable parameter and the corresponding value of the concrete. Soil parameters are varied one at a time, on a wide range of values, well beyond a realistic distribution, to emphasize the different effects of each one. By analysing the plots of figures 8 and 9, it may be deduced that

- For increasing values of the terrain stiffness both the frequency and the amplitude of the peak response increase.
- For an increasing value of the terrain density the peak response decreases while its frequency location remains unchanged.
- If the terrain has some flexibility the system's resonant frequency is always lower than the rigid case, regardless of terrain density (Figure 8).

As expected, the asymptotic response for very stiff terrain converges to the rigid foundation model (black dashed line).

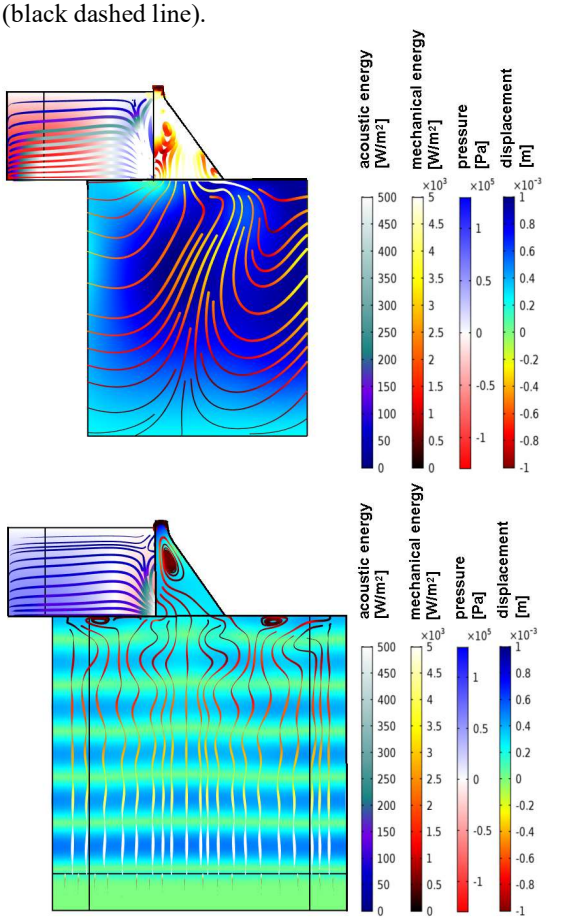

Figure 7. Displacement, pressure and mechanical energy flux streamlines plot for massless (top) and infinite massed terrain (bottom).

A further parametric study is performed. To this purpose, 625 parameter sets have been selected and COMSOL's *LiveLink*™ for MATLAB functionality has been used. Each set is made up of 4 values that are relative to the stiffness and the density of soil and dam concrete. The response curves are in terms of base resultant shear and each graph highlights a specific parameter variation (Figure 10). The colour bar expresses the ratio between the parameter value and the reference value reported in Table 1.

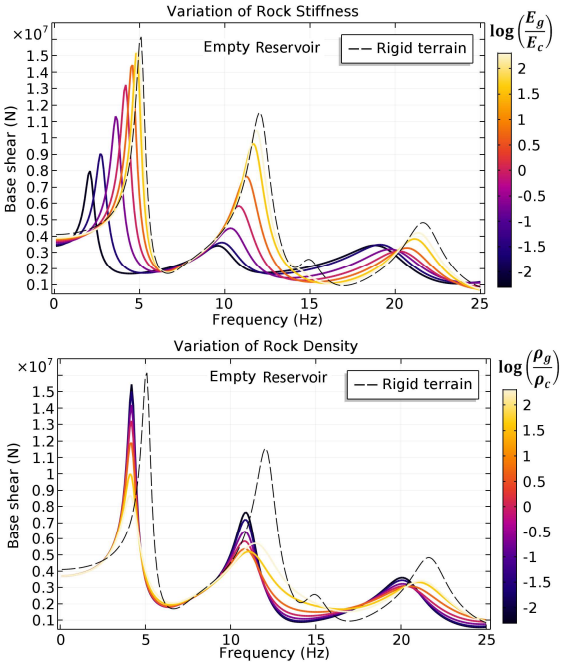

Figure 8. base shear response curves –variation of rock density and stiffness.

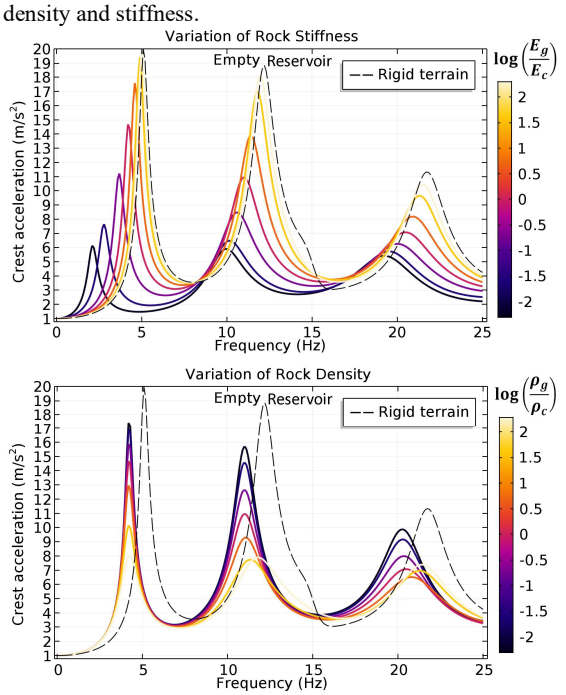

Figure 9. Crest acceleration response curves – variation of rock density and stiffness.

In Table 2 the variation intervals for each parameter are shown. The first and the last plot of figure 10 display a colour gradient, meaning a monotonic variation of the peak height and frequency position with rock stiffness and concrete density values, while the other two plots show a cross relationship and a stepped variation.

Parameter	*Minimum*	*Maximum*
$\mathbf{E_c}$ *(MPa)*	16447	24671
$\mathbf{E_g}$ *(MPa)*	17569	26353
$\boldsymbol{\rho_c}$ *(kg/m³)*	2014	3021
$\boldsymbol{\rho_g}$ *(kg/m³)*	1840	2760

Table 2. parameters variation range.

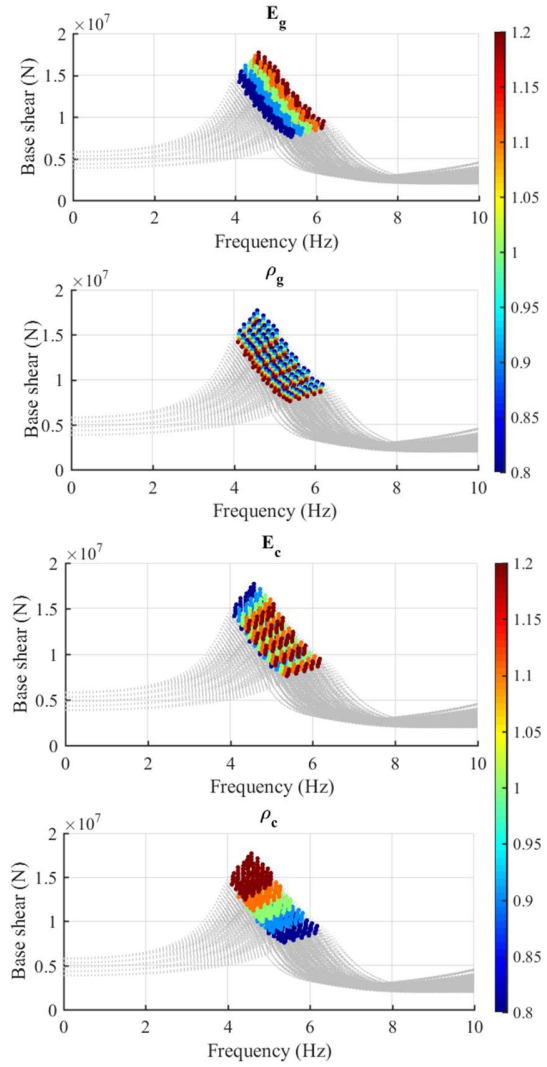

Figure 10. Parametric variation of peak shear, the color bar indicates each of the parameters ratio to the reference value in Table 1.

5. Damping estimation

In order to get a quantitative representation of the peak response attenuation due to radiation damping in the terrain, the response curves were analysed and the equivalent damping of the system is calculated via the half power bandwidth method.

The usual implementation of damping in finite element Solid Mechanics is done by the damping

matrix $[C]$ which can be expressed as a function of the stiffness matrix $[K]$ and the *loss factor* η

$$[\mathrm{C}] = (1 + \mathrm{i} \cdot \eta)[\mathrm{K}] \qquad (4)$$

For a Single Degree of Freedom system (SDOF), η is related to its frequency response function

$$\eta = \frac{\Delta \mathrm{f}}{\mathrm{f_r}} \cong 2\xi, \qquad (5)$$

where f_r is the resonant frequency, Δf is the frequency range where the response amplitude is higher than $\frac{a_p}{\sqrt{2}}$, with a_p the peak response amplitude, and ξ is the damping ratio. By analogy with a SDOF system, η can be evaluated for the first peak response. To this aim, the *findpeaks* command of MATLAB post-processing is used. In Table 3 the equivalent damping is reported for each case, along with the first peak frequency and the maximum value of the base shear.

	Freq. *(Hz)*	Loss factor η	Equivalent damping ξ	Peak shear *(N)* x10^7
Empty				
Rigid	6.83	9.78%	4.89%	2.336
Massless	4.49	10.94%	5.47%	2.887
Unbounded	5.19	23.11%	11.56%	0.870
Added masses				
Rigid	5.33	4.95%	2.48%	3.597
Massless	3.77	8.18%	4.09%	4.761
Unbounded	4.39	13.77%	6.89%	2.274
Interaction				
Rigid	5.62	9.47%	4.74%	6.639
Massless	3.79	9.04%	4.52%	5.490
Unbounded	4.37	17.23%	8.62%	2.871

Table 3. Equivalent damping for the different cases.

It can be seen that the material damping factor of 5% assigned to the domain is substantially reproduced by the rigid and massless models. Its value increases in the unbounded model. In particular, it ranges from two to three times the damping of the rigid case, with a maximum value of 23% in the empty reservoir case. This value decreases in the added mass models, while it is slightly higher in the acoustic coupled interaction, displaying a radiation effect also in the reservoir. This is confirmed by the noticeable reduction of the peak base shear in the unbounded case, which ranges from 37% in the rigid case and empty reservoir to 63% and 43% for the added masses and full interaction cases respectively.

η is also evaluated for the parametric sweeps in the empty reservoir case (Figure 11). The system damping decreases with the terrain stiffness, showing an asymptote at η = 10%, and increases with terrain density.

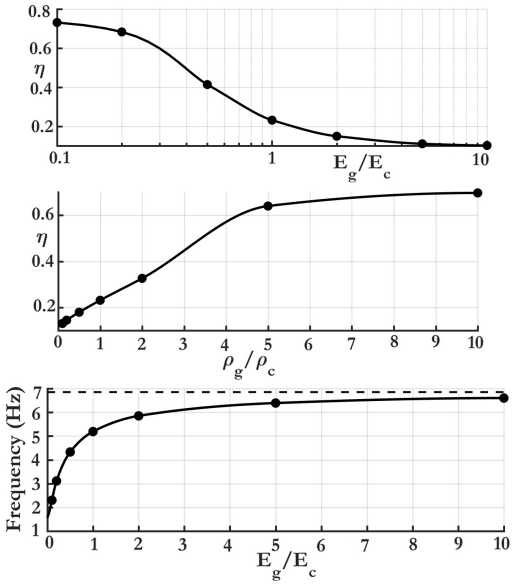

Figure 11. Equivalent soil loss factor vs. soil stiffness and density (first two plots); peak frequency vs. E_g/E_c (bottom).

6. Parametric analysis with full reservoir

The same parametric analysis displayed in the figures 8 and 9 is repeated in the case of fluid-structure interaction. Figures 12 and 13 report the response curves of resultant base shear and crest displacement, varying the soil stiffness E_g and its density ρ_g and keeping the corresponding values for the concrete unchanged (Table 1).

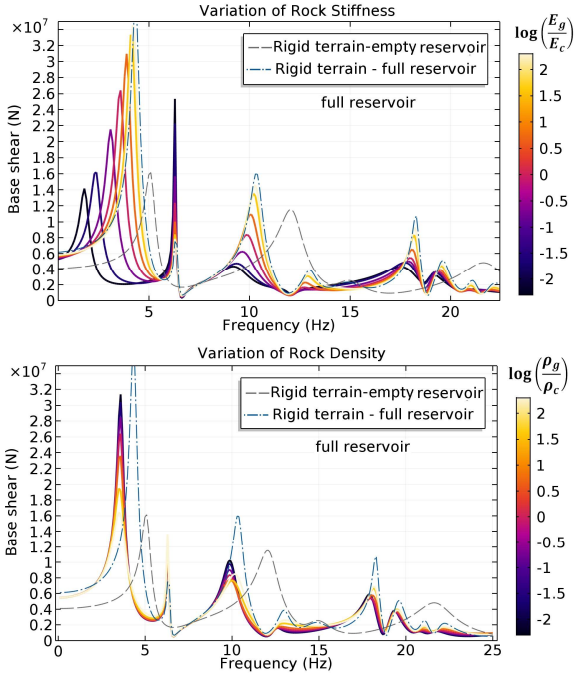

Figure 12. Parametric variation of base shear response curve with soil relative stiffness and density (full reservoir).

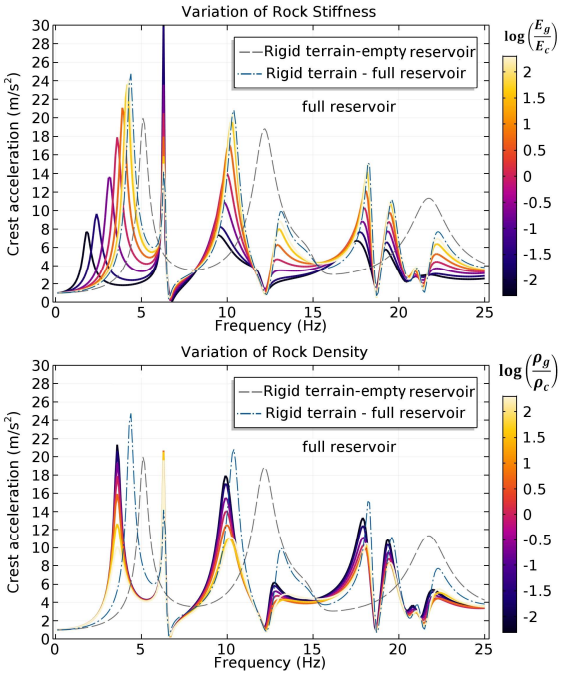

Figure 13. Parametric variation of crest acceleration response curve with soil relative stiffness and density (full reservoir).

In this case, the peak relative to the first frequency of the basin is evident and its presence is even more noticeable with increasing density and decreasing stiffness.

7. Conclusions

The main contribution of this work is to compare the results in terms of frequency response of different models, in order to take into account the effect of the unbounded soil half-space. COMSOL provides the needed tools in this regard, allowing the approximate determination of the resulting system damping, in presence of the radiation damping effect.

8. References

1. COMSOL Multiphysics®, User's Guide, Version 5.3, (2017).
2. E.L. Wilson, *Three-Dimensional Static and Dynamic Analysis of Structures, A Physical Approach With Emphasis on Earthquake Engineering,* Computers and Structures, Inc., Berkeley, California (2002).
3. J.P. Wolf, *Dinamic Soil Structure Interaction*, Englewood Cliffs, Prentice-Hall, New Jersey NJ (1985).
4. J.P. Wolf, C. Song, Some cornerstones of dynamic soil-structure interaction, *Engineering Structure* **24** 13-28 (2002).
5. R.W. Clough, Non-linear mechanisms in the seismic response of arch dams, *Proceedings of the Int. Conf. on Earthquake Engineering, Skopje, Yugoslavia* (1980).
6. A.K. Chopra, Earthquake analysis of arch dams: factors to be considered. *Proceedings of the 14th World Conference on Earthquake Engineering*, Beijing, China, (2008).
7. H. Lamb, On the Propagation of Tremors over the Surface of an Elastic Solid, Philosophical Transactions of the Royal Society of London. Series A, **203**, 1–42 (1903).
8. J. Lysmer, R.L. Kuhlemeyer, Finite dynamic model for infinite media, *J. Eng. Mech.*, *ASCE,* **95**(4), 859-878 (1969).
9. V. Lofti, J.L. Tassoulas, J.M. Roesset, A technique for the analysis of dams to earthquakes, *Earth. Eng & Struct. Dyn.* **15**(4) 463 – 489 (1987).
10. D.K., Kim, C.B. Yun, Time domain soil-structure interaction analysis in two dimensional medium based on analytical frequency-dependent infinite elements, *Int. J. Numer. Meth. Eng.*, **47**, 1241-1261 (2000).
11. C.B. Yun, D.K. Kim, J.M. Kim, Analytical frequency-dependent infinite elements for soil-structure interaction analysis in two-dimensional medium, *Engineering Structures*, **22**(3), 258-271 (2000).
12. G. Feltrin, *Absorbing boundaries for the time-domain analysis of dam-reservoir-foundation systems.* Report Swiss Federal Institute of Technology Zurich (1997).
13. M. Yazdchi, N. Khalili, S. Valliappan, Nonlinear seismic behaviour of concrete gravity dams using coupled finite element-boundary element technique. *International Journal for Numerical Methods in Engineering,* **44**(1), 101–130 (1999).
14 C. Song, J.P. Wolf, The scaled boundary finite-element method, a primer: solution procedures, *Comput. Struct.*, **78**, 211-225 (2000).
15. D. Givoli, High-order local non-reflecting boundary conditions: a review, *Wave. Mot.*, **39**, 319-326 (2004).
16. J.P. Berenger, A perfectly matched layer for the absorption of electromagnetic waves, J. *Comput. Phys.*, **114**, 185-200 (1994).
17. R.L. Kuhlemeyer, J. Lysmer., Finite Element Method Accuracy for Wave Propagation Problems. *Journal of the Soil Dynamics Division*, **99**, 421-427 (1973).
18. H. M. Westergaard, Water pressures on dams during earthquakes, *Trans. ASCE*, **98**, 418-433 (1933).